



HAL
open science

Evaluating the L-MEB Model From Long-Term Microwave Measurements Over a Rough Field, SMOSREX 2006

Arnaud Mialon, Jean-Pierre Wigneron, Patricia de Rosnay, Maria-José
Escorihuela, Yann H. Kerr

► **To cite this version:**

Arnaud Mialon, Jean-Pierre Wigneron, Patricia de Rosnay, Maria-José Escorihuela, Yann H. Kerr. Evaluating the L-MEB Model From Long-Term Microwave Measurements Over a Rough Field, SMOSREX 2006. IEEE Transactions on Geoscience and Remote Sensing, 2012, 50 (5), pp.1458-1467. 10.1109/TGRS.2011.2178421 . hal-00690897

HAL Id: hal-00690897

<https://hal.science/hal-00690897>

Submitted on 25 Apr 2012

HAL is a multi-disciplinary open access archive for the deposit and dissemination of scientific research documents, whether they are published or not. The documents may come from teaching and research institutions in France or abroad, or from public or private research centers.

L'archive ouverte pluridisciplinaire **HAL**, est destinée au dépôt et à la diffusion de documents scientifiques de niveau recherche, publiés ou non, émanant des établissements d'enseignement et de recherche français ou étrangers, des laboratoires publics ou privés.

Evaluating the L-MEB model from long term microwave measurements over a rough field, SMOSREX 2006

Arnaud Mialon, Jean-Pierre Wigneron, *Senior Member 03, IEEE*, Patricia de Rosnay, Maria Jose Escorihuela, Yann H. Kerr, *Member 88, Senior Member 01, IEEE*

Abstract—The present study analyses the effects of the roughness on the surface emission at L-band, based on observations acquired during a long term experiment. At the SMOSREX (Surface Monitoring Of the Soil Reservoir EXperiment) site near Toulouse, France, a bare soil was ploughed and monitored over more than a year by means of a L-band radiometer profile soil moisture and temperature sensors as well, as a local weather station, accompanied by 12 roughness campaigns. The aim of this study is (1) to present this unique database, and (2) to use this dataset to investigate the semi-empirical parameters for the roughness in L-MEB (L-Band Microwave Emission of the Biosphere), that is the forward model used, in the SMOS (Soil Moisture and Ocean Salinity) soil moisture retrieval algorithm. In particular, we studied the link between these semi empirical parameters and the soil roughness characteristics expressed in terms of standard deviation of surface height (σ) and the correlation length (LC). The dataset verifies that roughness effects decrease the sensitivity of surface emission to soil moisture, an effect which is most pronounced at high incidence angles and soil moisture and at horizontal polarization. Contradictory to previous studies, the semi-empirical parameter Q_r was not found to be equal to 0 for rough conditions. A linear relationship between the semi-empirical parameters N and σ was established, while N_H and N_V appeared to be lower for a rough ($N_H \sim 0.59$ and $N_V \sim -0.3$) than for a quasi-smooth surface. This study reveals the complexity of roughness effects and demonstrates the great value of a sound long-term dataset of rough L-band surface emissions to improve our understanding on the matter.

Index Terms—SMOS, Roughness, Passive Microwave, L-band, L-MEB model.

I. INTRODUCTION

SOIL moisture is a key parameter controlling air-land interface exchanges. Although very

important in many applications (climate models, agriculture, water resources management), it is difficult to monitor this variable at a global scale. The SMOS (Soil Moisture and Ocean Salinity) satellite mission [1; 2], successfully launched in November 2009, is the first mission to deliver global surface soil moisture fields at a high temporal resolution of 3 days. The retrieval scheme to derive soil moisture [3] is based on multi-angular passive microwave brightness temperatures ($f=1.4$ GHz) as measured by the instrument [4] and on surface emission models at L-band (L-MEB, L-band Microwave Emission of the Biosphere [5; 6; 7]).

Land surface emission at this wavelength is mainly controlled by soil moisture but important issues are still to be tackled [8] such as roughness, which is the focus of this paper. Roughness influence on surface emission is complex as it implies 3-D geometric soil surface features as well as soil moisture heterogeneity, in particular between peaks and hollows. Its major effect is to decrease the sensitivity of L-band brightness temperatures to soil moisture [9; 10]. Shi et al. [11] found by the use of an Integral Equation Model (IEM) that roughness influence is more significant at high incidence angles and high soil moisture content as well as a function of polarization. They noted an increase in emissivity with roughness at the horizontal polarization at low incidence angles. For dry soil, the emissivity of the vertical polarization (typically higher than ~ 0.8) shows a decrease compared with that of a flat surface, whereas for wet soil (emissivity lower than ~ 0.8) an increase is observed.

Using complex models as the IEM approach to compute the surface emissivity is not possible in the SMOS soil moisture algorithm as it needs many inputs and its computation is time demanding. Instead the SMOS level2 retrieval algorithm [3] uses semi-empirical approaches [7; 8] to compute the emission of the surface. The correction for a rough surface [9; 10; 12; 13]

A.Mialon and Y.Kerr are with the Centre d'Etudes Spatiales de la Biosphère (CESBIO), Toulouse Cedex 4, France.

P. de Rosnay is also with the CESBIO and presently at the European Centre for Medium-Range Weather Forecasts (ECMWF), Reading, UK.

J.P. Wigneron is with the Institut National de Recherche Agronomique (INRA), Bordeaux, France.

M.J Escorihuela is with isardSAT - Earth Observation Applications- Barcelona.

is based on empirical parameters (H_r , N_V , N_H , Q_r) that have to be calibrated with in-situ data reflecting local surface characteristics (soil texture level of roughness). Most recent studies on L-band emission [14; 15; 16] have retrieved these parameters to best fit the observations, but more investigations are needed on roughness to relate the soil L-MEB parameters to the surface roughness characteristics.

The roughness analyses conducted so far have all been either restricted to short investigation periods [17; 13] or to almost flat surface conditions [18] only. These have motivated the present study which for the first time focuses on a rough soil observed over a long time period at the SMOSREX (Surface Monitoring Of the Soil Reservoir EXperiment) site in 2006/07. A bare soil was ploughed creating a very rough surface and its roughness evolved over more than a year naturally due to climatic events (rainfalls, wind).

The aim of this study is twofold. First, this unique database (referred to as SMOSREX-2006) is presented and the L-band observations over the rough surface covering a wide range of soil moisture conditions (from very wet to very dry) are analysed over a long period of time (14 months). Second, the SMOSREX-2006 is used to evaluate the roughness parameters of the semi empirical model used in the L-MEB model. Q_r , H_r and N_V (p for the polarization horizontal or vertical) are retrieved in this evaluation and compared with the surface roughness characteristics.

II. MATERIAL

A. Database and experimental site

In preparation of the SMOS mission, the experimental site of SMOSREX (Surface Monitoring Of the Soil Reservoir EXperiment [19]) has been set up near Toulouse in the Southwest of France. Operating since 2003, the database has been used to improve the models implemented in the SMOS soil moisture retrieval [3; 20; 18].

It is equipped with the LEWIS (L-band radiometer for Estimating Water in Soil) radiometer [21], which has been continuously monitoring the emission of the surface. The instrument, placed on a 15m high tower can monitor two fields one with grasscover and a bare soil. It acquires brightness temperatures at vertical and horizontal polarizations (commonly referred to as V and H) at the same frequency as SMOS, i.e. 1.4 GHz, at several incidence angles (i.e. 20, 30, 40, 50 and 60°) every 3 hours (i.e. 2h30, 5h30, 8h30, 11h30,

14h30, 17h30, 20h30, 23h30 UTC).

Additionally, ground measurements are available. Soil texture was analysed and the bare soil was found to be 17% clay, 36% sand and 47% silt [19]. The SMOSREX site is equipped with a weather station, which has been monitoring meteorological data (air temperature, pressure, precipitation, wind) and soil moisture and temperature profiles are measured on each field every 30 minutes. Temperatures measured at different depths, i.e. at 1cm, 5cm, 20cm, 50cm and 90cm with one probe per depth, at the same location as the soil moisture probes, are used to compute the soil temperature. Surface soil moisture is obtained by averaging data from 5 probes placed at the surface (top 0-6 cm layer) on the bare soil field. Soil moisture probes are calibrated from gravimetric measurements [22], from which soil density is estimated.

It is important to note that obtaining an accurate estimation of soil moisture is difficult and can be slightly different from what contributes to the brightness temperatures measured by the radiometer. Due to surface heterogeneity, some differences can occur between the surface covered by the probes ($\sim 4m^2$) and LEWIS field of view that covers a wider surface [19]. Moreover, peaks and hollows imply strong heterogeneity in the surface soil moisture conditions, as soil water content is generally higher in hollows than on peaks. Finally, soil moisture probes measure the dielectric constant over the 0-6 cm top soil layer, whereas the surface emission in L-band is expected to be correlated to the soil moisture of the top 2-3 cm soil layer [23].

B. Roughness measurements

The roughness experiment took place on the bare soil field. On January 13th, 2006 the field was ploughed in a deep manner to ensure a distinct row structure parallel to LEWIS plane of incidence. Thereafter, surface roughness changed naturally over time in response to climatic events, mainly rainfalls and wind.

Surface roughness is measured by means of a two meter long needle board with 201 needles at 1 cm spacing. The needles move freely in the vertical direction and were allowed to fall till they touched the surface reproducing surface variations. Twelve measurement campaigns were conducted over the following 14 months (see Table I), each consisting in the acquisition of several roughness profiles (up to 6), in both directions, i.e. parallel and perpendicular to the plane of incidence of

the LEWIS instrument. Pictures of each vertical profiles were taken with a digital camera to obtain the corresponding numerical profiles of the height variation. These were then used to derive two statistical parameters describing the surface, the standard deviation of heights σ and the correlation length LC [24]. The daily σ are obtained by averaging the variance, i.e. σ^2 , of the different samples acquired in both directions. LC was derived from the auto-correlation function $C(x)$, Eq. 1 [24; 25], which measures the correlation between two heights separated by a distance x :

$$C(x) = \frac{\sum_{i=1}^{N+1-j} z_i \cdot z_{j+1-i}}{\sum_{i=1}^N z_i^2} \quad (1)$$

where $z(i)$ is the height of the needles; j integer ≥ 1 ; the spatial displacement $x=(j-1) \cdot \delta x$; δx being the distance between 2 needles, i.e. 1 cm; N the number of needles $N=201$. The LC corresponds to the distance x where the correlation function (Eq. 1) has decreased to $1/e$, i.e. beyond which two heights are no longer statistically correlated [24]. The auto-correlation function is commonly approximated by the function $C(x)=\exp\left(\frac{-|x|^n}{LC^n}\right)$ where $n=1$ for the Exponential model or $n=2$ for the Gaussian model [26; 25; 27]. For each day of measurement LC is simply the average of the different profiles, mixing both directions. For example, a flat surface is characterized by a low σ and a high LC.

Data acquired before this campaign, i.e. in February and April 2004 [18] and in January 13th just before ploughing the soil, are also used as they provide additional information concerning a quasi-smooth surface. Roughness was also measured in 2010 so that the soil roughness temporal variation could be estimated at interannual scale.

III. METHODOLOGY

A. Observations

The first part of our study is dedicated to surface emission at L-band as observed by the LEWIS radiometer. All cases such as freezing, snow storm on January 28-30 2006) that may introduce artefacts are excluded from the dataset. It is more pertinent to study surface emissivity than brightness temperature as the latter is also influenced by the soil temperature. The emissivity ϵ of a bare soil is obtained from the measured brightness temperatures by removing surface temperature and the sky contributions by applying the following $\epsilon_p = (TB_p - TB_{sky}) / (T_{eff} - TB_{sky})$, where the subscript p stands for the polarization (H or V), and T_{eff}

the effective soil temperature [28] as computed from measured temperatures at all depths based on [19; 29]. The sky contribution T_{sky} is quite low at L-band and set to a constant value of 3.7 K according to [21; 30].

To study the effect of surface roughness on the measured signal, the prevailing surface conditions are divided into four classes of differing σ . Ranges of σ are defined from a trend of measured σ (Eq. 5) to better emphasize the effect of roughness on the signal. The evolution of σ with time (Table I and Fig. 1) suggests the following ranges : $\sigma < 16$ mm relative to smooth surface, i.e. before the campaign ; σ belonging to the range 16-20 mm characterizing the steady state reached by the surface at the end of the campaign, from the end of April 2006 to March 2007 ; σ between 20 and 24 mm for the transition between very rough and steady state surface, from February to April 2006 ; and a last case concerning a very rough surface characterized by a σ higher than 24 mm, just after ploughing.

B. Surface modeling

This database is also used to retrieve and study the semi-empirical parameters in the L-MEB that account for the effect of a rough surface [3; 7]. The emission of a flat surface is obtained by computing its dielectric constant from soil conditions, i.e. texture, temperature and surface soil moisture. The model developed by Mironov et al. [31; 32] is used as it has been shown to be more relevant for our experiment site [23] than the Dobson's model [33; 34]. The reflectivity $\Gamma = 1-\epsilon$, is then derived using Fresnel's law for a flat soil. The surface emission, or reflectivity, must then be corrected to take into account a rough air-soil interface. This roughness contribution is estimated by the following semi-empirical approach [10; 17; 18]:

$$\Gamma_p(\theta) = [(1 - Qr) \cdot \Gamma_p^0(\theta) + Qr \cdot \Gamma_q^0(\theta)] \cdot e^{-Hr \cdot \cos^{N_p}(\theta)} \quad (2)$$

where Γ is the reflectivity with the subscripts p and $q = V$ or H for the Horizontal and Vertical polarizations; the index 0 stands for reflectivity of a flat surface computed from the Fresnel's law; θ being the incidence angle; Qr , Hr , N_p are the roughness parameters to be calibrated [10; 17]. Qr is a mixing factor that allows us to take into account the polarization mixing caused by the rough surface, N_p allows us to account for the incidence angle [35] and depends on the polarisation [18] and Hr is the effective roughness parameter.

292 A first attempt to relate these empirical
 293 parameters to surface roughness suggested that
 294 $Hr = (2k\sigma)^2$ [9]. Hr was also found to depend
 295 on soil moisture [17; 18; 14] but as it has not
 296 been confirmed [23], it is not considered in the
 297 present study. This dependence could be partially
 298 explained by a mismatch between sampling depth
 299 of soil moisture sensors and the actual depth
 300 of the surface emission layer in L-band [23].
 301 N_p ($p = H$ or V for horizontal and vertical
 302 polarization) was found to be different for the two
 303 polarizations and $N_H=1$ and $N_V=-1$ were found
 304 for our SMOSREX site [18]. Q_r is generally
 305 considered to be negligible [14; 15; 13; 18] at
 306 L-band but in reality a rough surface implies
 307 mixing in polarization [10; 26] that can only be
 308 simulated by setting $Q_r > 0$ [11].

309
 310 Parameter retrieval:
 311 4 parameters are unknown in Eq. 2, that are Q_r , Hr ,
 312 N_H and N_V . The retrieval is done in two steps. The
 313 first one is based on a relationship between N_H
 314 and N_V [18]. Indeed, both theory using Fresnel
 315 law and observations over a flat surface show that
 316 the reflectivity at H and V polarizations are related
 317 by the following approximate equation (see [18])
 318

$$\Gamma_H(\theta) = [\Gamma_V(\theta)]^{\cos^{AN}(\theta)} \quad (3)$$

319 For a smooth surface, ΔN (Eq. 3), i.e. the
 320 difference ($N_H - N_V$), was found to be equal to
 321 2 [18] which is not relevant for a rough surface
 322 [11]. $\Gamma_H(\theta)$ and $\Gamma_V(\theta)$ are extracted from our
 323 database (i.e. LEWIS measurements) for each day
 324 of the roughness campaign (see Table I, left hand
 325 column) allowing us to compute ΔN for rough
 326 conditions. The second step uses Eq. 2 from Lewis
 327 brightness temperatures, where $N_H - N_V$ are linked
 328 together as a results of the first step.

329 The retrieval consists of minimizing a cost function
 330 that computes the quadratic differences between
 331 measured emissivities (ϵ_{lewis} at incidence angles
 332 of $\theta = 20, 30, 40, 50^\circ$ and both polarizations)
 333 and simulated emissivities (ϵ_{model}). This sets the
 334 best values of parameters (Eq. 2) that fit the
 335 observations [3] [5]. The cost function to be
 336 minimized is:
 337

$$CF = \frac{\sum (\epsilon_{lewis} - \epsilon_{model})^2}{\delta(\epsilon_{lewis})^2} + \sum_i \frac{\sum (P_i^{init} - P_i)^2}{\delta(P_i^2)} \quad (4)$$

338 where ϵ_{lewis} at all angles and polarizations
 339 are used; $\delta(\epsilon_{lewis})$ being the error in emissivity
 340 measured by LEWIS instrument [21]; P_i are

the retrieved parameters (Q_r , Hr , and N_p), P_i^{init}
 the initial values of the retrieved parameters
 (respectively $Q_r^{init} = 0.1$, $Hr^{init} = 0.75$, $N_p^{init} = 1$);
 and $\delta(P_i)$ the standard deviation of the retrieved
 parameters ($\delta Q_r = 1$, $\delta Hr = 2$, $\delta N_H = 1$).

As Q_r was found to be = 0 [13], two cases are
 considered here: A) where $Q_r = 0$ and Hr , N_H and
 N_V are retrieved and B) all the 4 parameters Q_r ,
 Hr , N_H and N_V are retrieved.

IV. RESULTS AND DISCUSSION

This section presents the results obtained from
 the SMOSREX-2006 campaign. Firstly, roughness
 measurements are presented for 14 months and
 secondly, the emissivities measured by the LEWIS
 instrument are analyzed to better understand
 the effect of roughness on the L-band surface
 emission. Finally, this database is used to study the
 semi empirical model that accounts for roughness
 in L-MEB. The parameters of the semi-empirical
 model are derived and related to surface roughness
 conditions.

A. Measured roughness

Table I presents the means and standard
 deviations of σ and LC as well as the ratio σ/LC
 acquired during σ each day of the campaign. Mean
 values are obtained considering samples at both
 orientations, i.e. parallel and perpendicular to
 LEWIS plane of incidence. Before ploughing,
 the surface was almost flat characterized by
 $\sigma=4.73\pm 1.31$ mm and a correlation length $LC =$
 94.11 ± 38.81 mm. As a comparison, previous
 measurements of the SMOSREX site [18] reported
 $\sigma = 11.09$ mm in February 2004 and $\sigma = 9.12$ mm
 in April 2004, indicating a smooth surface. After
 ploughing, the surface was characterized by a
 standard deviation height σ of $34.58 \text{ mm} \pm 10.29$
 mm and a correlation length of 62.42 ± 26.68 mm.
 The auto-correlation functions (Eq. 1) suggest that
 the surface is closer to an exponential one than a
 gaussian one [26; 27].

The time variations of σ (top panel), the cor-
 relation length (2^{nd} panel from the top), the soil
 moisture (3^{rd} panel from the top) from the end of
 2005 to March 2007 and the emissivity monitored
 at an incidence angle of 40 at both polarizations
 (bottom panel) are given in Fig. 1. The effects
 of the soil ploughing can be clearly distinguished
 on January 13th (top panel) and is characterized

TABLE I
STANDARD DEVIATION OF HEIGHTS, σ , AND THE CORRELATION LENGTH, LC, FOR EACH DAY OF THE CAMPAIGN. σ AND LC ARE AVERAGED FROM EVERY SAMPLES ACQUIRED AT BOTH DIRECTIONS. THE RIGHT-HAND COLUMN IS THE RATIO σ /LC

| date Year mm/dd/yy | Roughness Characteristics | | |
|--------------------------|---|-------------------------------|----------------------|
| | Standard Deviation of surface height σ (mm) | correlation length LC (mm) | σ /LC (mm) |
| 02-07-03* | 11.51* \pm 2.72 | 59.56* \pm 35.90 | 0.19* |
| 02-04-04* | 11.09* \pm 3.59 | 101.22* \pm 42.20 | 0.11* |
| 04-02-04* | 9.12* \pm 2.18 | 70.67* \pm 33.70 | 0.13* |
| 01-13-06* | 4.73* \pm 1.31 | 94.11* \pm 38.81 | 0.05* |
| 01-13-06 | 34.58 \pm 10.29 | 62.42 \pm 26.68 | 0.55 |
| 01-20-06 | 29.67 \pm 9.66 | 70.21 \pm 29.55 | 0.42 |
| 02-01-06 | 26.85 \pm 11.17 | 60.99 \pm 16.90 | 0.44 |
| 02-20-06 | 25.58 \pm 5.86 | 65.26 \pm 22.88 | 0.39 |
| 03-16-06 | 23.10 \pm 6.61 | 76.06 \pm 33.78 | 0.30 |
| 04-03-06 | 25.44 \pm 6.76 | 87.78 \pm 34.97 | 0.29 |
| 05-04-06 | 20.93 \pm 7.05 | 96.08 \pm 56.66 | 0.22 |
| 05-30-06 | 20.32 \pm 7.22 | 82.39 \pm 31.60 | 0.25 |
| 06-29-06 | 18.05 \pm 4.84 | 105.19 \pm 43.16 | 0.17 |
| 11-24-06 | 19.25 \pm 5.99 | 118.21 \pm 33.12 | 0.16 |
| 03-12-07 | 17.43 \pm 5.72 | 115.32 \pm 42.66 | 0.15 |
| 10-06-10 | 12.31 \pm 3.19 | 122.68 \pm 62.42 | 0.10 |

* Measurements before ploughing

393 by a sharp increase in σ followed by a noticea24
394 ble decrease in σ from January to May. Then σ 5
395 decreases more slowly, reaching a quasi-constant6
396 value by July 2006. After 14 months σ was about7
397 17.4 mm. In June 2010 the soil roughness was mea28
398 sured (Table I) and presented a level of roughness9
399 comparable with the value measured in April 2004,30
400 as $\sigma=12.31\pm 3.19$ mm and $LC=122.68\pm 62.42$ mm31
401 This trend is well reproduced using an exponential32
402 fit function (dashed line top panel Fig. 1) as: 433

$$\sigma = 38.35xDOE^{-0.126} \quad (434)$$

403 with DOE being the Day of the Experiment (dashed36
404 line top panel Fig. 1). The correlation length 437
405 LC- presents an opposite behaviour, showing a low38
406 value after ploughing and increasing with time as39
407 the surface becomes less and less rough. A fit40
408 function was used to represent its trend (dashed41
409 line, 2nd panel from top Fig. 1) and is defined as42

$$LC = 48.67xDOE^{0.132} \quad (443)$$

410 The effect of ploughing leads to a decrease in4
411 soil moisture as shown in Fig. 1 (2nd Fig. from45
412 the bottom) in January 2006. This effect could be46
413 explained by a redistribution of the water content47
414 within the soil. Consequently, the emissivity48
415 (bottom panel of Fig. 1) increases whereas the49
416 difference of polarization, $\epsilon_V - \epsilon_H$, decreases. It50
417 should be noted that ploughing changes also the51
418 bulk density: the soil density decreasing from52
419 1.5 kg/m³ in 2005, to 1.39 kg/m³ in February53
420 20th, 2006. Weather conditions then compact the54
421 surface, decreasing σ and increasing the density to55
422 1.57 kg/m³ in November 2006. Thus, ploughing56
423 the surface modifies the soil properties (bulk57

density, soil moisture redistribution) impacting the
dielectric constant and so the surface emissivity
[17].

σ and LC are correlated as seen in Fig. 2, which
reports the relation existing between LC, σ /LC and
 σ^2 /LC as a function of σ . Estimating LC from field
measurements is difficult (i.e. the measurements
are noisy) but a modeling study [36] has shown
that it has a very low influence on brightness
temperature, especially at H polarization. The
results of σ and LC are slightly different to what
was obtained with the same database [26] as their
methodology to compute σ and LC is different.

B. Observations of surface emissivities

Fig. 3 presents the emissivity calculated from
LEWIS measurements as a function of soil moisture
at 4 incidence angles, from $\theta=20^\circ$ (top row)
to $\theta=50^\circ$ (bottom row) and for both polarizations
(V black dots and H grey dots). The different
columns correspond to the four roughness classes
from quasi-smooth on the right to rough surfaces on
the left. Emissivity computed from Fresnel's law is
plotted (grey and black lines Fig. 3) characterizing
the emission of a perfectly smooth surface with
identical surface conditions (i.e. with the same
soil moisture, density, temperatures). As expected,
emissivity decreases with increasing soil moisture
at both polarizations and all angles. The effect of
roughness is to decrease the sensitivity of surface
emission to soil moisture. This can be observed
especially at wet conditions (i.e. $> 0.25m^3/m^3$),
where the emissivity increases with roughness. The

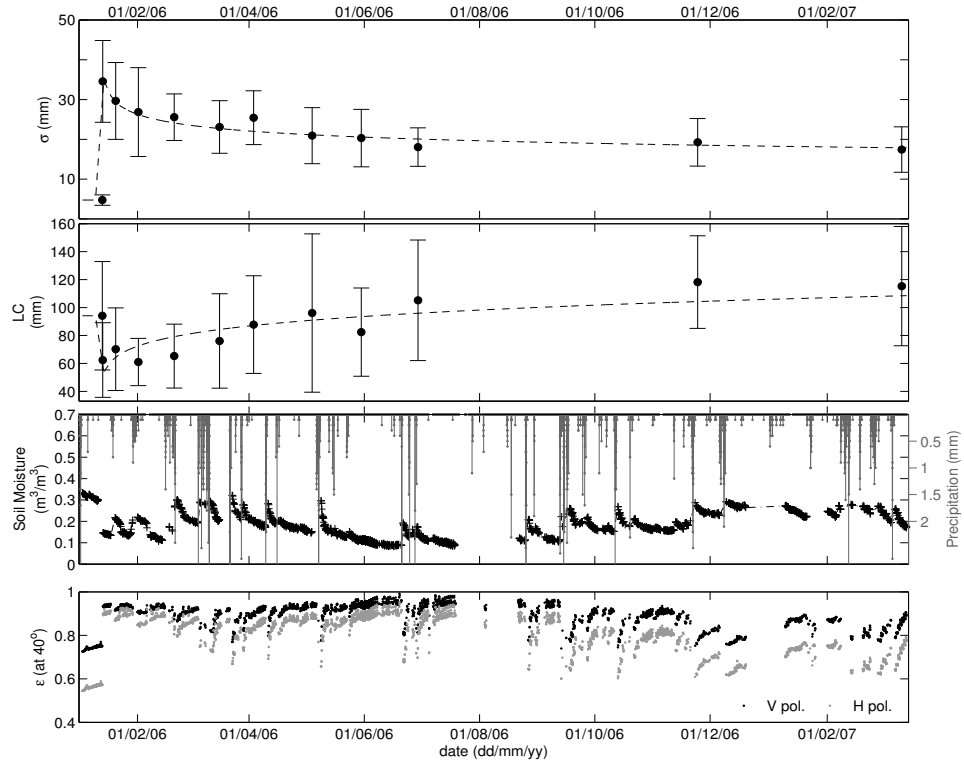


Fig. 1. Time series of surface parameters from December 2005 to March 2007. Top Fig. is σ (in mm) and its standard deviation ; The surface was ploughed the 13th of January 2006. 2nd from the top: the correlation length ; 3rd panel: soil moisture (black x, left hand y-axis) and precipitation (grey sticks, right hand y-axis, note that it is inverted for graphical convenience) ; Bottom figure is the emissivities at V (black dots) and H (grey dots) polarizations monitored by Lewis radiometer at an incidence angle of 40° .

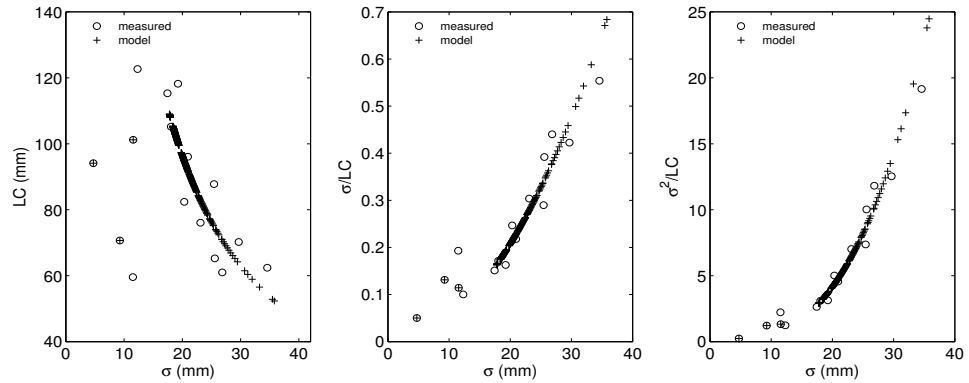


Fig. 2. LC , σ/LC and σ^2/LC as a function of σ . For each case are displayed: the measured σ and LC (Table I), “o” symbols and referred to as “measured” in the legends; σ and LC obtained from Eq. 5 and 6, “+” symbols and referred to as “modeled” in the legends. Measured and model data are similar for data acquired before ploughing the surface.

458 difference between the emissivities at H and V pol-
 459 arization increases with increasing incidence angle
 460 for each wetness conditions but is decreased with
 461 roughness. Furthermore, the impact of roughness
 462 on the emissivity is more pronounced at H than
 463 V polarization. At the incidence angle of 40° , the
 464 emissivity at H pol. is ~ 0.56 at a soil moisture
 465 content of $0.3m^3/m^3$ and for a smooth surface (3rd
 466 line, right hand side Fig. 3) whereas it is ~ 0.8 for a
 467 rough surface (left hand side Fig. 3). It corresponds

to an increase in the emissivity of 0.24, whereas for
 the V polarization this increase is ~ 0.145 , from an
 emissivity of ~ 0.72 for flat condition to ~ 0.865 for
 a rough surface. The decrease in the emissivity with
 soil moisture has a linear trend for rough conditions
 and for each incidence angle (left-hand columns
 Fig. 3), the effect being again more pronounced at
 H polarization than at V polarization.

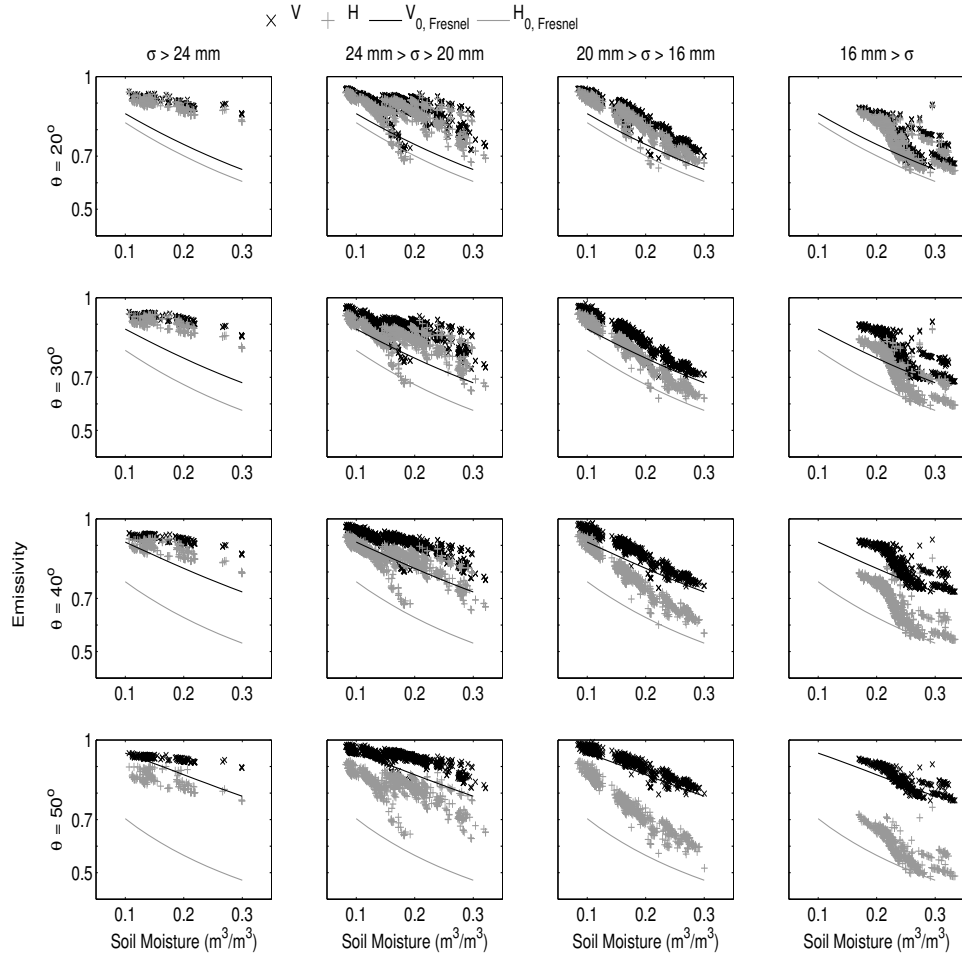


Fig. 3. Emissivity at V (black x) and H (grey +) polarizations, monitored at 4 incidence angles as a function of soil moisture : 20° (top row figures), 30° (2nd row), 40° (3rd row) and 50° (bottom row). The 4 columns correspond to roughness conditions, from a very rough surface -1st column from the left- to quasi-smooth condition (right hand side column). Emissivity computed from Fresnel's law (flat surface) is shown as black (V pol.) and grey (H pol.) continuous lines.

476 C. L-Meb model calibration

477 The second objective of this paper is to use the
478 database to study the roughness parameters (Q_r ,
479 H_r , N_H and N_V) as defined in Eq. 2.

480
481 1) Relation between N_H and N_V : ΔN is derived
482 from Eq. 3 and presented in Fig. 4 as a function of
483 σ values estimated by the fit function (Eq. 5 and
484 grey dashed line Fig. 1). The use of the fit instead
485 of actual values is done to limit errors caused by
486 sampling limits in characterizing the field (2196
487 board and ~ 8 samples per day). Fig. 4 clearly
488 shows a decreasing trend of ΔN with σ , well
489 represented by the linear function defined as ΔN
490 $= N_H - N_V = -0.049 \cdot \sigma + 2.188$ ($R = 0.90$, $RMSE$
491 $= 0.16$, $bias=0$). Smoother surface, i.e. $\sigma < 16$
492 mm, is characterized by a ΔN of ~ 1.8 , which is
493 in agreement with $\Delta N = 2$ found previously [18]
494 whereas it is ~ 0.5 for very rough surface, i.e. $\sigma > 24$
495 35mm. This trend is close to that obtained in [13]

496 ($\Delta N = -0.036 \cdot \sigma + 2.24$) over another agricultural
site.

2) Retrieved parameters: N_p ($p= H$ or V), Q_r
and H_r (Eq. 2) were derived from Eq. 4, for every
day over the period November 2005-April 2007.
The emissivity computed using these parameters,
leads to an $RMSE=0.022$ ($R^2=0.95$) when compared
to LEWIS emissivity, whereas an $RMSE = 0.053$
($R^2=0.69$) is encountered when applying the
parameters found by Escorihuela et al. [18] over a
flat surface. Fig. 5 presents the retrieved roughness
parameters Q_r (top Fig.), H_r (middle Fig.) and
 N_H and N_V (bottom Fig.) for case B as a function
of time. The time variation in σ and its best fit
trend (Eq. 5) are also showed for comparison. H_r
presents a high variability, but in general it decreases
as σ decreases.

The high variability in the retrieved values of
 H_r could be linked to the fact that this parameter

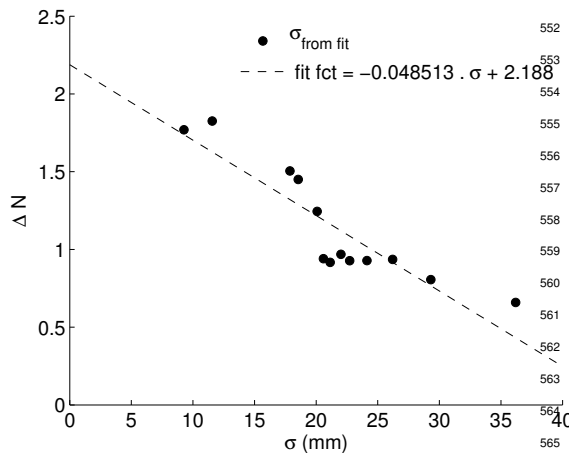


Fig. 4. σ estimated from roughness measurements plotted against ΔN (black \bullet) calculated from LEWIS data, including the linear fit function (dashed line).

tends to compensate for the difference between the sampling depth [23] [37] of the in-situ soil moisture sensors ($\sim 0-6$ cm top soil layer) and of the LEWIS observations ($\sim 0-2/3$ cm). For example after a rain event following dry soil moisture conditions, the LEWIS observations immediately show a clear decrease in the monitored brightness temperatures whereas the in-situ probe still measures a low water content. Whilst LEWIS is sensitive to the first 0-2/3 cm, which is wet after a rain event, the probe integrates the soil moisture between the surface layer which is wet and a deeper layer which is dryer. In this case, the soil moisture estimated by the probe is underestimated in comparison to the soil moisture seen by LEWIS. The L-MEB model uses this underestimated soil moisture and compensates this effect by adjusting H_r to fit the LEWIS observations. Such effects may explain the high variability in the retrieved values of H_r obtained in May, July, September 2006. The opposite situation is also observed (dry surface over the 0-2/3 cm surface layer and rather wet conditions over the 0-6 cm surface layer) and could explain high retrieved values of H_r obtained in March 2004 and November 2005.

The results of the retrieval are presented as a function of the estimated σ (Eq. 5, dashed line top Fig. 1) and LC (Eq. 6) in Fig. 6 and Fig. 7 (grey markers for the case A with $Q_r=0$ and black markers for the case B where Q_r is retrieved). We also studied the derived parameters with the quantity σ/LC (not shown here), but the results are very similar to the results presented in Fig. 6. Q_r (case B, it is retrieved, black \bullet Top left Fig. 6) increases significantly from values around 0.05 for

a flat surface to 0.3 for a rough surface. A Low Q_r value for a quasi-smooth surface is in agreement with both theory (no polarization mixing, [11]) and observations [13] [18]. It confirms also that Q_r is not equal to 0 for rough surface and needs to be taken into account to model the signature of rough soils. Retrieved values of H_r (Top right Fig. 6) show more variability as mentioned earlier. They evolve on average from $\sim 0.2-0.3$ for a smooth surface to ~ 1 for a rough surface. The relation $H_r=f(\sigma)$ obtained in [13] is represented by the dashed line, fitting the results of the presented study. It is interesting to note that this relationship obtained for different conditions over a different site and a variety of soil roughness conditions provide a good general fit to the results obtained in this study. These results confirm that the empirical relationship $H_r = (2k\sigma)^2$ [9] (dotted line Fig. 6) is not applicable, also found in [13]. Retrieved values of H_r when Q_r , H_r and N_p ($p = H$ or V) are retrieved are higher than when Q_r is set equal to 0. Q_r and H_r variations seem to be correlated to variations in σ whereas no clear correlation with σ could be found for N_V and N_H (bottom left Fig. 6) confirming the observations of [13]. N_H and N_V are found on average to be equal to 2.8 and 1 respectively for a smooth surface whereas the authors of [18] set them to lower values of 1 and -1. For rough surface however, N_H and N_V do not vary and can clearly be set to $N_H=0.59$ and $N_V=-0.30$. Q seems related to H_r (bottom right Fig. 6) by the relation $H=2.69*Q$ ($R=0.71$). Eq. 2 imposes the conditions $Q=0$ for $H=0$, meaning the emissivity of a flat surface is that from Fresnel's law.

The retrieved parameters show the opposite behavior when studied as a function of LC (Fig. 7) with H_r and Q decreasing with increasing LC. N_V and N_H present less variations for a rough surface (low LC) than in Fig. 6.

V. CONCLUSIONS AND PERSPECTIVES

Roughness effects at L-band are complex and need more investigations to be fully understood and modeled [13; 38]. This paper presents the unique SMOSREX-2006 experimental database dedicated to study the effect of roughness at L-band over 14 months. A bare soil has been significantly ploughed at the SMOSREX site and continuously monitored by LEWIS L-band radiometer. It has been found that the influence of roughness is more important at high incidence angles (about 40 to 50°), high soil moisture values and at H polarization.

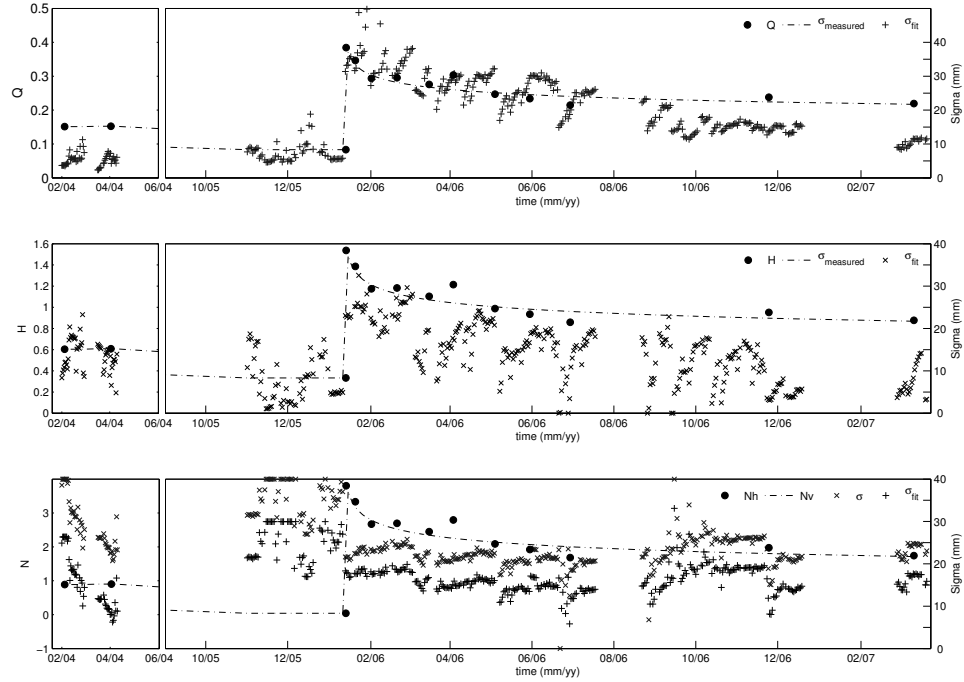


Fig. 5. Time series of the roughness parameters of Eq. 2. Top figure shows Q_r , middle figure shows H_r and the bottom figure presents N_H (x) and N_V (+). σ and its fit trend (Eq. 5) are also depicted (with right hand side y-axis). The time series are split in two panels (left and right hand columns) as the time series are not continuous (no roughness measurement in 2005).

607 The soil moisture derived from the SMOS₆
 608 mission is based on a semi-empirical approach₇
 609 [8] and the roughness effect is taken into account₈
 610 by the Q-H model [9; 13; 18]. The presented₉
 611 database is also used to study the semi-empirical₀
 612 parameters of the L-MEB emission model as a₁
 613 function of surface characteristics represented₂
 614 by σ and LC. The results of this study suggest₃
 615 that for a rough surface $Q_r=0.3$, $H_r \sim 1$, $N_H \sim$
 616 0.59 and $N_V \sim -0.30$, whereas a smooth surface₅
 617 is characterized by $Q_r \sim 0.05$, $H_r \sim 0.2/0.3$, N_H
 618 ~ 2.8 and $N_V \sim 1$. It is different from most of
 619 the previous works on the subject which set $Q=0$
 620 even for rough conditions. A simple model can
 621 not have been found to represent the dependence₈
 622 of the semi-empirical parameters with σ and LC₉
 623 due to their high variability, especially in case₀
 624 of H_r . However, it is interesting to note that₁
 625 the σ - H_r relation proposed by [13] seems to be₂
 626 applicable here over SMOSREX conditions. A
 627 linear relationship between N_H and N_V is also₃
 628 found, with the difference $N_H - N_V$ decreasing₄
 629 with σ . The variations of these semi-empirical₅
 630 parameters can be explained by the difference₆
 631 in sampling depth between the sensors that are₇
 632 not sensitive to the same surface layer. This₈
 633 difference can be reduced by selecting some₉
 634 certain weather and soil moisture conditions.
 635 After an important rainfall the soil reaches its₀

field capacity and is more homogeneous in terms
 of soil moisture content as both the 0-2/3 cm
 top layer (as monitored by LEWIS) and the top
 0-6cm (as monitored by the probes) should have
 the same soil moisture content. After a drying
 period, the soil reaches its lower soil moisture
 content and both the probes and LEWIS monitor
 the same amount of soil moisture. By extracting
 those specific periods, it is expected to reduce the
 variability of the derived parameters.

ACKNOWLEDGMENT

The authors would like to thank the SMOSREX
 partners Météo-France and ONERA. This ex-
 periment was funded by Programme National de
 Télédétection Spatiale and Terre Océan Surfaces
 Continentales et Atmosphère.

REFERENCES

- [1] Y. H. Kerr, "Soil moisture from space: Where are we?" *Hydrogeology Journal*, vol. 15, pp. 117–120, 2007.
- [2] Y. H. Kerr, P. Waldteufel, J.-P. Wigneron, J. Font, and M. Berger, "Soil moisture retrieval from space : the soil moisture and ocean salinity (smos) mission," *IEEE T. Geosci. Remote*, vol. 39(8), pp. 1729–1735, 2001.

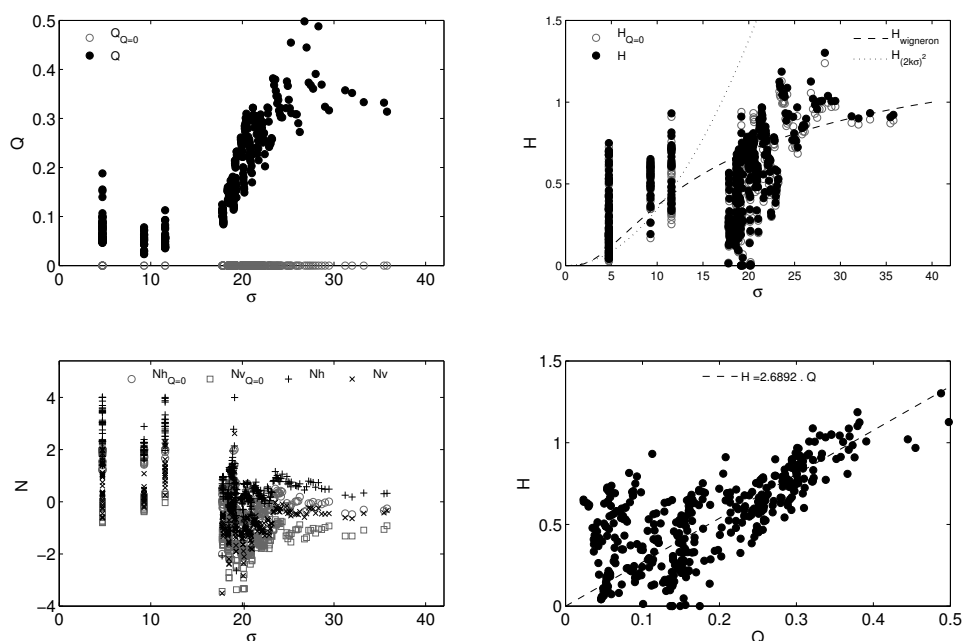


Fig. 6. Retrieved Q_r , H_r and N_p ($p=V$ or H) as a function of estimated σ (i.e. Eq. 5). Two cases considered : A) $Q_r=0$, H_r and N_p ($p=V$ or H) are derived (grey markers on all Figure); B) Q_r is derived (black markers). In the top right figure are also depicted H functions as found in i) Wigneron et al. 2011 [13] (dashed line) and ii) $H_r = (2k\sigma)^2$ [9] (dotted line).

- 662 [3] Y. H. Kerr, P. Waldteufel, P. Richaume, J.-P. Wigneron, P. Ferrazzoli, and R. Gurney, "SMOS level 2 processor for soil moisture - Algorithm Theoretical Based Document (ATBD)," CBSA, Tech. Rep. SO-TN-ESL-SM-GS-0001, Issue 3.e, 2011, 126 p. [Online]. Available: <http://www.cesbi-ups-tlse.fr/fr/indexsmos.html>
- 663
664
665
666
667
668
669
- 670 [4] Y. H. Kerr, J. Font, P. Waldteufel, A. Camps, J. Bara, I. Corbella, F. Torres, N. Duffo, M. Vall-llossera, and G. Caudal, "Next Generation radiometers: SMOS a dual pole L-band 2D aperture synthesis radiometer," P. Pampaloni and S. Paloscia, Eds., *Utrecht The Netherlands*, pp. 447–483, 2000.
- 671
672
673
674
675
676
677
- 678 [5] J.-P. Wigneron, J.-C. Calvet, T. Pellarin, A. Van de Griend, M. Berger, and P. Ferrazzoli, "Retrieving near surface soil moisture from microwave radiometric observations: Current status and future plans," *Remote Sens. Environnement*, vol. 85, pp. 489–506, 2003.
- 679
680
681
682
683
- 684 [6] J.-P. Wigneron, J.-C. Calvet, P. de Rosnay, Y. H. Kerr, P. Waldteufel, K. Saleh, M. J. Escorihuela, and A. Kruszewski, "Soil moisture retrievals from biangular L-band passive microwave observations," *Geoscience and Remote Sensing Letters IEEE*, vol. 1(4), pp. 277–281, 2004, doi=10.1109/LGRS.2004.834594.
- 685
686
687
688
689
690
691
- 700 [7] J.-P. Wigneron, Y. H. Kerr, P. Waldteufel, K. Saleh, M.-J. Escorihuela, P. Richaume, P. Ferrazzoli, P. de Rosnay, R. Gurney, J.-C. Calvet, J. P. Grant, M. Guglielmetti, B. Hornbuckle, C. Mätzler, T. Pellarin, and M. Schwank, "L-band Microwave Emission of the Biosphere (L-MEB) Model : Description and calibration against experimental data sets over crop fields," *Rem. Sens. Environ.*, vol. 107, pp. 639–655, 2007.
- 710 [8] Y. H. Kerr, P. Waldteufel, P. Richaume, A. Mahmoodi, J.-P. Wigneron, P. Ferrazzoli, A. Al bitar, F. Cabot, D. Leroux, A. Mialon, and S. Delwart, "The SMOS soil moisture retrieval algorithm," *IEEE Geosc. Remote Sens.*, 2011, submitted.
- 720 [9] B. Choudhury, T. Schmugge, A. Chang, and R. Newton, "Effect of surface Roughness on the microwave emission from soil," *J. Geophys. Res.*, vol. 84, no C9, pp. 5699–5706, 1979.
- 730 [10] J. R. Wang and B. J. Choudhury, "Remote sensing of soil moisture content over bare fields at 1.4 GHz frequency," *J. Geophys. Res.*, vol. 86, pp. 5277–5282, 1981.
- 740 [11] J. Shi, K. S. Chen, Q. Li, T. J. Jackson, P. E. O'Neill, and L. Tsang, "A parameterized surface reflectivity model and estimation of bare-surface soil moisture with L-band radiometer," *IEEE T. Geosci. Re-*

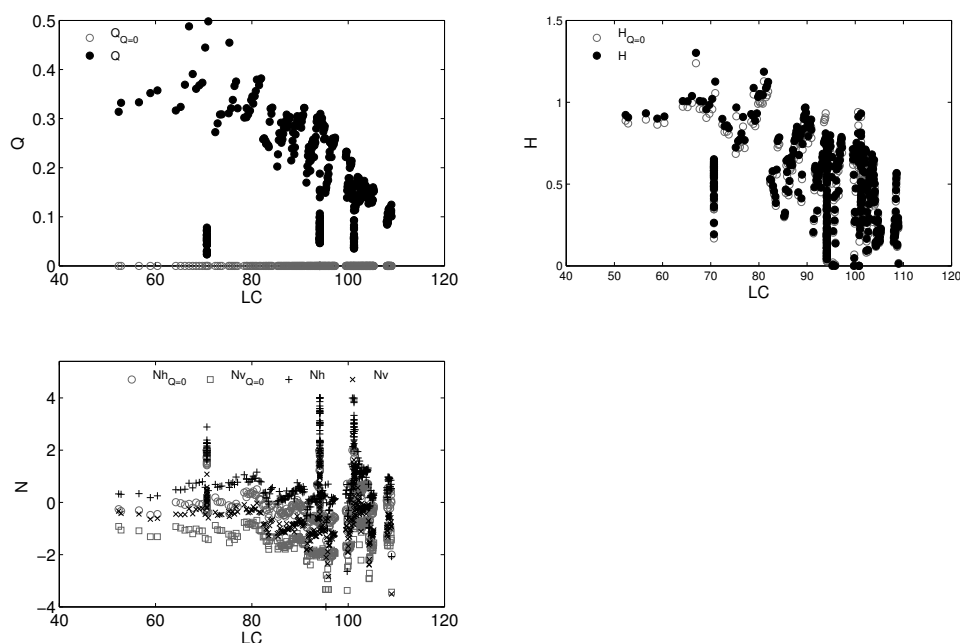
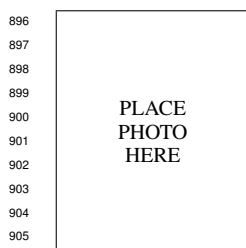


Fig. 7. Retrieved Q_r , H_r and N_p ($p=V$ or H) as a function of estimated LC (i.e. Eq. 6). Two cases considered : A) $Q_r=0$, H_r and N_p ($p=V$ or H) are derived (grey markers) B) Q_r is derived (black markers on all Fig.).

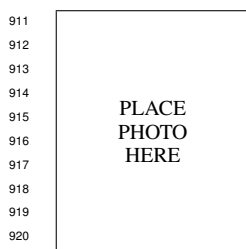
- 722 *mote*, vol. 40 (no 12), pp. 2674–2686, 2002, doi=10.1109/TGRS.2002.807003. 754
- 723
- 724 [12] J. R. Wang, P. E. O’Neill, T. J. Jackson, and E. T. Engman, “Multifrequency measurements of the effects of soil moisture, soil texture and surface roughness,” *IEEE Trans. Geosci. Remote Sensing*, vol. 21, pp. 44–51, 1993. 756
- 725
- 726
- 727
- 728
- 729 [13] J.-P. Wigneron, A. Chanzy, Y. H. Kerr, H. Lawrence, J. Shi, M.-J. Escorihuela, V. Mironov, A. Mialon, F. Demontoux, P. de Rosnay, and K. Saleh-Contell, “Evaluating an Improved Parameterization of the Soil Emission in L-MEB,” *IEEE Geosci. Remote Sensing Letters*, vol. 49 (4), pp. 1175–1189, 2010, doi=10.1109/TGRS.2010.2075935. 760
- 730
- 731
- 732
- 733
- 734
- 735
- 736
- 737 [14] R. Panciera, J. P. Walker, J. Kalma, E. J. Kim, K. Saleh, and J.-P. Wigneron, “Evaluation of the SMOS L-MEB passive microwave soil moisture retrieval algorithm,” *Remote Sensing of Environment*, vol. 113, no. 2, pp. 435 – 444, 2009, doi:10.1016/j.rse.2008.10.010. 761
- 738
- 739
- 740
- 741
- 742
- 743 [15] K. Saleh, Y. H. Kerr, P. Richaume, M. J. Escorihuela, R. Panciera, S. Delwart, G. Boulet, P. Maisongrande, J. P. Walker, P. Wursteisen, and J.-P. Wigneron, “Soil moisture retrievals at L-band using a two-step inversion approach (COSMOS/NAF’05 Experiment),” *Remote Sensing of Environment*, vol. 113, no. 6, pp. 1304 – 1312, 2009, doi=10.1016/j.rse.2009.02.013. 762
- 744
- 745
- 746
- 747
- 748
- 749
- 750
- 751
- 752 [16] A. Cano, K. Saleh, J.-P. Wigneron, C. Antolín, J. E. Balling, Y. H. Kerr, A. Kruszewski, C. Millán-Scheidig, and S. Søbjaæg, “The smos mediterranean ecosystem l-band characterisation experiment (melbex-i) over natural shrubs,” *Remote Sensing of Environment*, vol. 114, no. 4, pp. 844 – 853, 2010, doi:10.1016/j.rse.2009.11.019. 763
- 764
- 765 [17] J.-P. Wigneron, L. Laguerre, and Y. H. Kerr, “A simple parameterization of the L-band microwave emission from rough agricultural soils,” *Geoscience and Remote Sensing, IEEE Transactions on*, vol. 39(8), pp. 1697–1707, 2001, doi=10.1109/36.942548. 766
- 767
- 768 [18] M. Escorihuela, Y. Kerr, P. de Rosnay, J. Wigneron, J. Calvet, and F. Lemaître, “A Simple Model of the Bare Soil Microwave Emission at L-Band,” *IEEE T. Geosci. Remote Sensing*, vol. 45 (vol 7, Part 1), pp. 1978–1987, 2007. 769
- 770
- 771 [19] P. de Rosnay, J. Calvet, Y. Kerr, J. Wigneron, F. Lemaître, M. Escorihuela, J. Sabater, K. Saleh, J. Barrié, G. Bouhours *et al.*, “SMOSREX: A long term field campaign experiment for soil moisture and land surface processes remote sensing,” *Remote Sens. Environ.*, vol. 102 (n 3-4), pp. p377–389, 2006. 772
- 773
- 774 [20] K. Saleh, J.-P. Wigneron, P. Waldteufel, P. de Rosnay, M. Schwank, J.-C. Calvet, and Y. H. Kerr, “Estimates of surface soil moisture under grass covers using l-band radiometry,” *Remote Sensing of Environment*, 775

- vol. 109, no. 1, pp. 42 – 53, 2007, doi:10.1016/j.rse.2006.12.002.
- [21] F. Lemaître, J.-C. Poussière, Y. H. Kerr, M. Dejus, R. Durbe, P. de Rosnay, and J.-C. Calvet, “Design and test of the ground-based L-band Radiometer for Estimating Water In Soils (LEWIS),” *IEEE T. Geosci. Remote*, vol. 42 (8), pp. 1666–1676, 2004, doi=10.1109/TGRS.2004.831230.
- [22] T. J. Schmugge, T. J. Jackson, and H. McKim, “Survey of methods for soil moisture determination,” *Water Resources Res.*, vol. 16(6), pp. 961–979, 1980, doi:10.1029/WR016i006p00961.
- [23] M. Escorihuela, A. Chanzy, J. Wigneron, and Y. H. Kerr, “Effective soil moisture sampling depth of l-band radiometry: A case study,” *Remote Sensing of Environment*, vol. 114, no. 5, pp. 995 – 1001, 2010, doi:10.1016/j.rse.2009.12.011.
- [24] F. T. Ulaby, R. K. Moore, and A. K. Fung, *Microwave remote sensing, active and passive*. Dedham, MA, USA : Artech house, 1986, vol. 2 : Radar Remote Sensing and Surface Scattering and Emission Theory.
- [25] N. E. C. Verhoest, H. Lievens, W. Wagner, J. Álvarez-Mozos, M. Moran, and F. Mattia, “On the soil roughness parameterization problem in soil moisture retrieval of bare surfaces from synthetic aperture radar,” *Sensors*, vol. 8, pp. 4213–4248, 2008, doi 10.3390/s8074213.
- [26] M. Schwank, I. Völsch, J.-P. Wigneron, Y. H. Kerr, A. Mialon, P. de Rosnay, and C. Mätzler, “Comparison of two Bare Soil Reflectivity Models and Validation With L-Band Radiometer Measurements,” *IEEE Trans. Geosci. Remote Sensing*, vol. 48(1), pp. 325–337, 2010, doi:10.1109/TGRS.2009.2026894.
- [27] H. Lawrence, J.-P. Wigneron, F. Demontoux, A. Mialon, and Y. H. Kerr, “Evaluation of a semi-empirical H-Q model, used to calculate the emissivity of a rough bare soil, with numerical modeling approach,” *IEEE Transactions on Remote Sens.*, 2011, submitted.
- [28] F. T. Ulaby, R. K. Moore, and A. K. Fung, *Microwave remote sensing, active and passive*. Dedham, MA, USA : Artech house, 1986, vol. 3 : From Theory to Applications.
- [29] P. de Rosnay, J. Wigneron, T. Holmes, and J. Calvet, “Parametrizations of the effective temperature for L-band radiometry. Inter-comparison and long term validation with SMOSREX field experiment,” in C. Mätzler (Eds) *Thermal microwave radiation - Applications for remote sensing*. London, UK: IEE Electromagnetic Waves Series, 2006.
- [30] T. Pellarin, J.-P. Wigneron, J.-C. Calvet, M. Berger, H. Douville, P. Ferrazzoli, Y. H. Kerr, E. Lopez-Baeza, J. Pulliainen, L. Simmonds, and P. Waldteufel, “Two-years global simulation of the L-band brightness temperature over land,” *IEEE T. Geosci. Remote*, pp. p2135–2139, 2003.
- [31] V. L. Mironov and S. V. Fomin, “Temperature and Mineralogy Dependable Model for Microwave dielectric Spectra of Moist Soils,” *PIERS Online*, vol. Vol. 5, N. 5, pp. 411–415, 2009, doi:10.2529/PIERS090220054025.
- [32] V. L. Mironov, L. G. Kosolapova, and S. V. Fomin, “Physically and mineralogically based spectroscopic dielectric model for moist soils,” *IEEE Trans. Geosci. Remote Sensing*, vol. Vol. 47, N. 7, pp. 2059–2070, 2009.
- [33] M. Dobson, F. Ulaby, M. Hallikainen, and M. El-Rayes, “Microwave dielectric behavior of wet soil-part ii: Dielectric mixing models,” *IEEE T Geosci. Remote*, vol. GE-23, no. 1, pp. 35–46, 1985.
- [34] N. Peplinski, F. Ulaby, and M. Dobson, “Dielectric properties of soils in the 0.3-1.3-GHz range,” *IEEE T. Geosci. Remote*, vol. 33, no. 3, pp. 803–807, 1995.
- [35] C. Prigent, J. Wigneron, W. Rossow, and J. Pardo-Carrion, “Frequency and angular variations of land surface microwave emissivities: can we estimate SSM/T and AMSU emissivities from SSM/I emissivities,” *IEEE T. Geosci. Remote*, vol. 38, pp. 2373–2386, 2000.
- [36] Q. Li, L. Tsang, J. Shi, and C. H. Chan, “Application of physics-based two-grid method and sparse matrix canonical grid method for numerical simulations of emissivities of soils with rough surfaces at microwave frequencies,” *Geoscience and Remote Sensing, IEEE Transactions on*, vol. 38, no. 4, pp. 1635 – 1643, 2000, doi : 10.1109/36.851963.
- [37] S. Raju, A. Chanzy, J.-P. Wigneron, J.-C. Calvet, Y. H. Kerr, and L. Laguerre, “Soil moisture and temperature profile effects on microwave emission at low frequencies,” *Remote Sensing of Environment*, vol. 54, no. 2, pp. 85 – 97, 1995, doi: 10.1016/0034-4257(95)00133-L.
- [38] H. Lawrence, F. Demontoux, J.-P. Wigneron, P. Paillou, T.-D. Wu, and Y. H. Kerr, “Evaluation of a Numerical Modeling Approach based on the Finite Element Method for calculating the Rough Surface Scattering and Emission

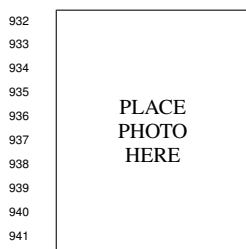
894 of a soil layer,” *IEEE TGRES letters*, 2011, in
895 press.



896 **Arnaud Mialon** Arnaud Mialon received the M.S. degree in climate and
897 physics-chemistry of the atmosphere in
898 2002 and a Ph.D. degree in ocean
899 atmosphere-hydrology from Université
900 Joseph Fourier de Grenoble (France)
901 and a Ph.D. in remote sensing from
902 the Université de Sherbrooke (Québec,
903 Canada) in 2005. He joined the Centre
904 d’Etudes Spatiales de la Biosphère,
905 Toulouse, France, in 2006. His fields
906 of interest are focused on passive microwave remote sensing
907 of continental surfaces. He has been involved in the SMOS
908 (Soil Moisture and Ocean Salinity) mission since 2006 and
909 in charge of the experimental site of SMOSREX since 2007.



911 **Jean-Pierre Wigneron** Jean-Pierre
912 Wigneron (SM 03) received the
913 Engineering degree from SupAéro
914 Ecole Nationale Supérieure
915 l’Aéronautique et de l’Espace
916 (ENSAE), Toulouse, France, in 1987
917 and the Ph.D. degree from University
918 of Toulouse, France, in 1993. He is
919 currently a Senior Research Scientist
920 at the Institut National de Recherche
921 Agronomiques (INRA), Bordeaux,
922 France, and the Head of the remote sensing group at EPHYSE,
923 Bordeaux. He coordinated the development of the L-MEB
924 model for soil and vegetation in the Level-2 inversion algorithm
925 of the ESA-SMOS Mission. His research interests are in
926 microwave remote sensing of soil and vegetation, radiative
927 transfer, and data assimilation. He was a Principal Investigator
928 of several international campaigns in the field of microwave
929 remote sensing. He has over 70 refereed papers in remote
930 sensing. He has been a member of the Editorial Board
931 Remote Sensing of Environment since 2005.



932 **Yann H. Kerr** Yann H. Kerr received
933 the engineering degree from ENSAE
934 the M.Sc. from Glasgow University
935 in E&EE, and Ph.D from Université
936 Paul Sabatier. From 1980 to 1985 he
937 was employed by CNES. In 1985 he
938 joined LERTS. He spent 19 months
939 working at JPL, Pasadena in 1987-88. He has been
940 working at CESBIO since 1995. His
941 fields of interest are in the theory and
942 techniques for microwave and thermal
943 infrared remote sensing of the Earth, with emphasis on hydrology,
944 water resources management and vegetation monitoring.
945 He was an EOS principal investigator (interdisciplinary investigations).
946 He was the science lead on the MIRAS project for ESA, and is now the
947 of the SMOS mission Lead-Investigator.



Patricia de Rosnay Patricia de Rosnay received her Ph.D degree in climate modelling from the University Pierre et Marie Curie (Paris 6, France) in 1999. She is currently Senior Scientist with the European Centre for Medium-Range Weather Forecasts (ECMWF) where is responsible of the land surface data assimilation activities. Her current research interests focus on improving soil moisture and snow analysis for Numerical Weather Prediction. She developed and implemented a 2-Dimensional Optimum Interpolation snow analysis and also implemented in operations an Extended Kalman Filter soil moisture analysis at ECMWF and she is investigating the use of passive and active microwave satellite data for Numerical Weather Prediction. She is involved in the SMOS Validation and Retrieval Team and participates to the EUMETSAT H-SAF project. She is member of the Science Definition Team and the Application Working Group of the future NASA SMAP mission and member of the SRNWP surface team. She was involved in land surface modelling activities such as the African Monsoon Multidisciplinary Analysis (AMMA) Land Surface Model Inter-comparison Project (ALMIP) and she coordinated the microwave component of the project ALMIP-MEM (Microwave Emission Model). She initiated the project for the validation of the future SMOS soil moisture products over West Africa. Patricia de Rosnay worked five years with the French Centre National de la Recherche Scientifiques (CNRS) at Centre d’Etudes Spatiales de la Biosphère (CESBIO), Toulouse, France, where she coordinated the SMOSREX field experiment in preparation of SMOS. Her research topic at the Laboratoire de Météorologie Dynamique (LMD) from 1994 to 2002 was focused on developments of global scale land surface processes representation in climate models.



Maria Jose Escorihuela Maria Jose Escorihuela received an Engineering degree in electronics and telecommunications from the Universitat Politècnica de Catalunya (UPC) in 1996 and a Ph. D. degree in Environmental, Space and Universe Sciences from the Institut National Polytechnique in Toulouse (France) in 2006. From 2003 to 2006, she was in the Centre d’Etudes Spatiales de la Biosphère (CESBIO) in Toulouse, France, where she developed models of natural surfaces emission at L-band for soil moisture estimation in the framework of the Soil Moisture and Ocean Salinity (SMOS) mission. In 2007 she was a visiting scientist in the Bureau of Meteorology Research Center (BMRC) in Melbourne (Australia) in the framework of a collaboration between the BMRC, the Melbourne University and the CESBIO for the analysis of experimental data over the SMOS cal/val sites. Since 2008, she is head of the Applications Department at isardSAT. Her scientific fields of interest are the application of passive and active microwave remote sensing to hydrology and climate change studies.